



HAL
open science

Defect-free ZnSe nanowire and nanoneedle nanostructures

Thomas Aichele, Adrien Tribu, Catherine Bougerol, Kuntheak Kheng, Régis André, Serge Tatarenko

► **To cite this version:**

Thomas Aichele, Adrien Tribu, Catherine Bougerol, Kuntheak Kheng, Régis André, et al.. Defect-free ZnSe nanowire and nanoneedle nanostructures. *Applied Physics Letters*, 2008, 93 (14), pp.143106. 10.1063/1.2991298 . hal-02547517

HAL Id: hal-02547517

<https://hal.science/hal-02547517>

Submitted on 18 May 2022

HAL is a multi-disciplinary open access archive for the deposit and dissemination of scientific research documents, whether they are published or not. The documents may come from teaching and research institutions in France or abroad, or from public or private research centers.

L'archive ouverte pluridisciplinaire **HAL**, est destinée au dépôt et à la diffusion de documents scientifiques de niveau recherche, publiés ou non, émanant des établissements d'enseignement et de recherche français ou étrangers, des laboratoires publics ou privés.

Defect-free ZnSe nanowire and nano-needle nanostructures

Thomas Aichele,* Adrien Tribu, Catherine Bougerol, Kuntheak Kheng, Régis André, and Serge Tatarenko

*Nanophysics and Semiconductor Group, CEA/CNRS/Université Joseph Fourier,
Institut Néel, 25 rue des Martyrs, 38042 Grenoble cedex 9, France*

(Dated: March 23, 2021)

We report on the growth of ZnSe nanowires and nano-needles using molecular beam epitaxy (MBE). Different growth regimes were found, depending on growth temperature and the Zn–Se flux ratio. By employing a combined MBE growth of nanowires and nano-needles without any post-processing of the sample, we achieved an efficient suppression of stacking fault defects. This is confirmed by transmission electron microscopy and by photoluminescence studies.

Semiconductor nanowires (NWs) have attracted much attention in recent years because of their properties and potential use in a variety of technological applications. NW heterostructures are interesting candidates for the development of well-located and size-controlled quantum dots (QDs) [1]. Due to the narrow lateral size, QD heterostructures in NWs can be directly grown on very defined positions and without the necessity of self-assembly. This is an especially interesting feature for II–VI materials, where self-assembled island formation occurs only within narrow windows of growth conditions [2]. Recently, II–VI compound semiconductor NWs have been synthesized by Au-catalysed metal-organic chemical vapour deposition (MOCVD) and molecular-beam epitaxy (MBE) methods [3, 4]. An obstacle towards the growth of optically active NW heterostructures are donor–acceptor pairs that form in defects [5]. These cause a strong spectral background which competes with the excitonic emission in the QDs. Ref. [6] reports the efficient reduction of this spectral background after annealing of the NW samples in Zn-rich atmosphere.

When developing NW heterostructures, annealing or other post-growth processing of the sample is often unfavourable as it may also influence the designed form of the heterostructure through inter-diffusion of the constituents. Instead, growth methods, that directly avoid the formation of defects are desired. In this letter, we report a growth recipe for ZnSe NWs, where the amount of stacking fault defects is strongly reduced. This was achieved by a combined growth of NWs and nano-needles without any post-growth processing of the sample.

The ZnSe NWs were grown in the vapour-liquid-solid growth mode with gold particles as catalysts. For comparison, GaAs(001) and Si(001) substrates were used. Degased surfaces for MBE growth were obtained after annealing in ultra-high vacuum at 580° C. In the case of GaAs, the effect of an epitaxial GaAs buffer layer was also investigated. Interestingly the structural properties of the NWs depend very little on the utilized substrate.

Next, a thin gold film with thickness of 0.2–0.5 nm was deposited on the GaAs substrates inside an electron beam metal deposition chamber. The gold film was dewetted to a droplet-like surface by annealing the sample at 600° C for 5 min. ZnSe MBE growth was then performed with varying growth conditions. The sample transfers between the MBE- and metal deposition chambers happened under ultra-high vacuum.

When growing under an excess of Se (Zn (Se) flux: 2.5 (7.5) $\times 10^7$ torr) and a sample temperature of 350–450° C, a dense carpet of narrow NWs with high aspect ratios covers the substrate. The NWs have a uniform diameter of 20–50 nm and a length up to 2 μm after a growth of one hour (fig. 1(a)). Additionally to the NWs, the as-grown substrate is covered with highly irregular nano-structures. Fig. 1(b) shows a transmission electron microscopy (TEM) image of one NW. The crystal structure of the NWs are predominantly wurtzite. However, the NWs are systematically intersected with regions of zinc blende phase. We account for the formation of such defects and the presence of highly irregular structures by non-ideal growth conditions at the initial stages of the growth process. Possible reasons are the presence of non-uniform gold agglomerations instead of small gold beads and the insertion of impurities during the gold deposition process. The presence of both wurtzite and Zn-blende shows, that at the utilized growth conditions both phases are allowed. Although, the observation of wurtzite structure is in contrast to the Zn-blende that naturally occurs in bulk ZnSe, it is not an uncommon behaviour for NWs, as discussed in ref. [7].

When, on the other hand, growing at low temperature (300° C) or with inverted Zn:Se flux ratio, needle-shaped NWs are formed (fig. 2(a)). Hereafter we will refer to those nanostructures as *nano-needles* to distinguish them from the narrow *NWs* described previously. By TEM (fig. 2(b)) we determined that the nano-needles have a wide base (80 nm in diameter) and a sharp tip (5–10 nm). We also observed darker and lighter regions which again indicate the presence of stacking fault defects. The formation of nano-needles instead of NWs is well accounted for by the slower adatoms mobility expected at low temperature or at low Se flux. The slower mobility promotes nucleation on the sidewalls before reaching the gold catalyst at the nano-needle tip. Moreover, we observed that the

*Corresponding author. E-mail: thomas.aichele@physik.huberlin.de; present address: Institut für Physik, Humboldt Universität zu Berlin, Hausvogteiplatz 5–7, 10117 Berlin, Germany

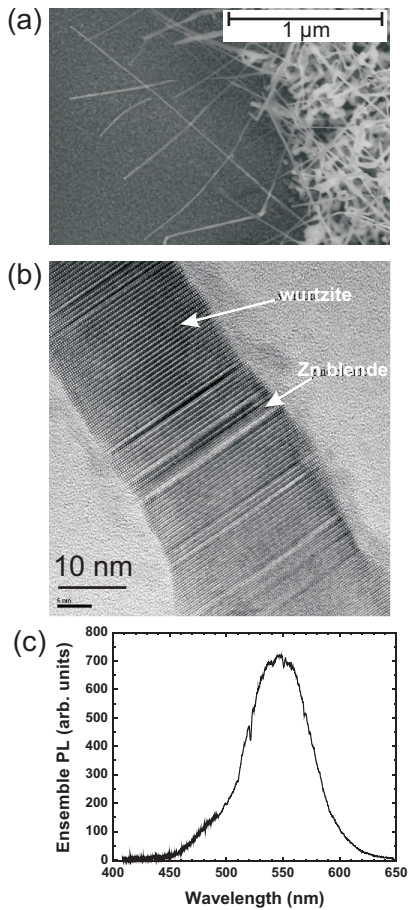


Figure 1: Data obtained from NWs grown at 400° C: (a) SEM image of the as-grown sample at the border of the gold-coated region. The right side shows the dense carpet of NWs. On the left, individual NWs reach into the uncoated zone. (b) TEM image of a single NW. The arrows indicate wurtzite and Zn-blende zones.

nano-needles are predominantly wurtzite, as for NWs, but the wire axis is here perpendicular to the *c*-axis instead of being parallel. In contrast also to the long NWs (in fig. 1), the defect planes are here disoriented with respect to the nano-needle axis. It seems that this disorientation hinders the propagation of defects in the growth direction, especially for lower diameters. Defects zones are rapidly blocked on the side walls, providing a high structural quality towards the nano-needle tip.

To carry out single-NW studies, the sample is put in a methanol ultra-sonic bath for 30 s in order to detach some NWs from the substrate. Droplets of this solution are next placed on a fresh substrate, leaving behind a low density of individual NWs. Ensemble spectra were taken on the as-grown sample. All spectra in this paper were measured at a sample temperature of 5 K. The photoluminescence (PL) of individual NWs were excited with a cw laser at 405 nm via a microscope objective.

Both for NWs and nano-needles, we observe a broad

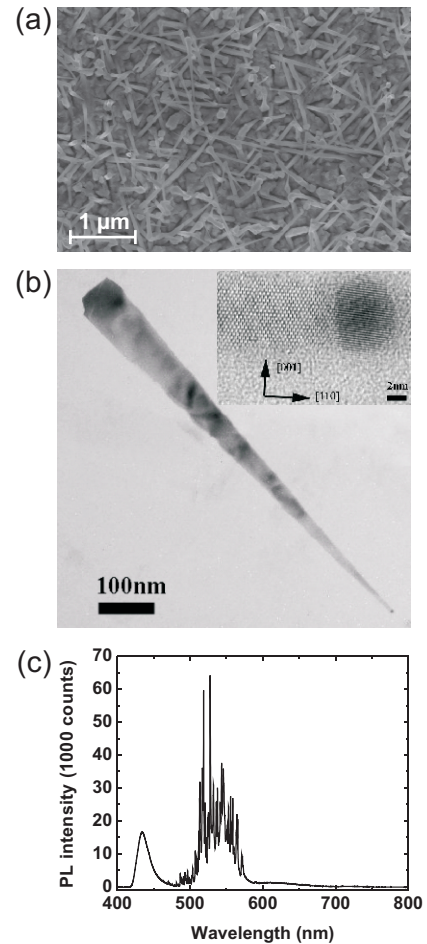


Figure 2: Data obtained from nano-needles, grown at 300° C at Se excess: (a) SEM of the as-grown sample. (b) TEM image of a single nano-needle. The inset shows a zoom to the region around the tip.

spectral distribution within 500–600 nm, as seen in figs. 4(a) and (b). Even in the case of a single nano-needle, the spectrum is dominated by many intense spectral lines, which we attribute to emission from excitons localized at the defect zones in the NW [5]. In contrast to the observations in ref. [6] on MOCVD-grown NWs, we do not see an enhancement of the ZnSe band edge emission (443 nm at 5 K [8]) when growing under Zn-rich conditions. The intense emission with 500–600 nm instead suggests that in both cases (NWs and nano-needles), point defects effectively capture the excited charge carriers and quench the band edge emission, as also reported in Ref. [9]. This is in agreement with the high density of stacking fault defects observed by TEM.

The observation of a decreasing defect density from the base towards the top in the nano-needles motivated us to modify the growth recipe in the following way: In the first part, the sample is grown with excess of Zn for 30 min, leading to the formation of nano-needle struc-

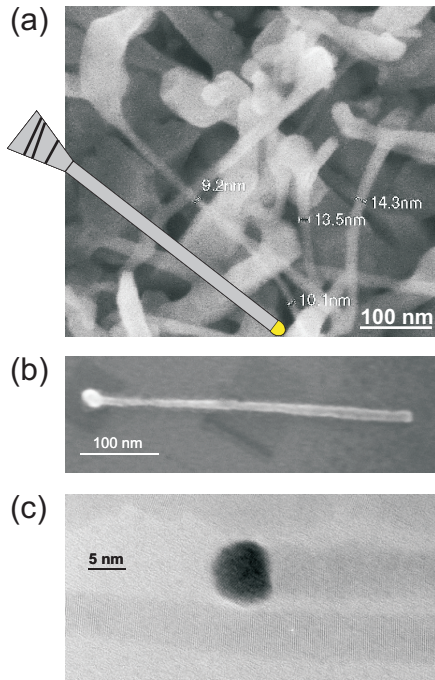


Figure 3: Data obtained from combined growth of NWs on nano-needle tips. (a) SEM image of the as-grown NW/nano-needle sample. (b) SEM of an isolated NW that broke off behind the thicker base. (c) TEM image of two close-by NWs.

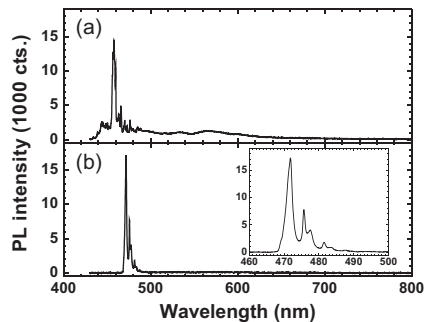


Figure 4: PL spectra from the different samples: (a) NW sample from fig. 1; (b) nano-needle sample from fig. 2; (c) and (d) combined NW/nano-needle sample from fig. 3. The inset of (d) is a zoom into the region 460–500 nm.

tures. Next, the Zn- and Se-flux was inverted and NWs were grown for another 30 min on top of the nano-needles. Thus, the growth at the side-walls was aborted and re-growth started on defect-free and strain-relaxed nano-needle tips, where the high structural quality of the crys-

tal lattice can be preserved along the narrow NW that is now formed in this second growth step. Fig. 3 shows results obtained from this sample. The structures have a broad base that tapers after a few ten nanometers to thin NWs with thickness of 10–15 nm. As symbolized in the sketch in fig. 3(a) we expect that stacking faults reduce towards the thin part of the NW, which is indeed the case, as seen in TEM images of a single NW, fig. 3(c).

The suppression of defects has a strong effect on the PL of these nano-structures (fig 4). Due to the low density of defects, the spectral emission between 500-600 nm that was observed before from the samples in figs 4(a) and (b) is strongly reduced, leaving behind only a small bunch of intense spectral lines between 450–500 nm. The weak and broad distribution between 500–600 that remains in the ensemble PL, fig 4(c), is due to excitons localized in defects in the thicker NW base. In the spectrum of a single NW that broke off behind the thicker base, fig 4(d), this broad background is now globally suppressed. In spite of this, no PL is observed at the ZnSe band-edge. A possible reason is that, due to the very thin diameter of the NWs, additional surface states may form in the bandgap [10] and introduce non-radiative decay channels that quench the band-edge PL. The remaining narrow PL peaks around 470 nm in fig. 4(d) can very likely be assigned to residual impurities responsible for donor-acceptor pair emission and their related phonon replica [11].

In summary we have reported on MBE growth of ZnSe NWs. Depending on growth temperature and Zn-Se flux ratio, we can tailor the structures between thin NWs with homogeneous thickness of 20–50 nm, and nano-needles with broad base and a sharp tip with 5–10 nm thickness. By combining nano-needle and NW growth, we achieved the growth of mostly defect-free structures, without any post-growth treatment of the sample. This is confirmed by TEM and PL measurements. In the latter, the emission of excitons localized in the defect zones was strongly reduced. The suppression of defects is an important pre-condition for developing QD heterostructures inside NWs. In a next step, we included CdSe zones into the NW in order to form QDs. This will be reported in a subsequent publication.

Acknowledgments

We are grateful to V. Zwiller for inspiring discussions. T.A. acknowledges support by Deutscher Akademischer Austauschdienst (DAAD).

- [1] M. T. Borgström, V. Zwiller, E. Müller, and A. Imamoglu, *Nanoletters* **5**, 1439 (2005).
 [2] I.-C. Robin, R. André, C. Bougerol, T. Aichele, and S.

- Tatarenko, *Appl. Phys. Lett.* **88**, 233103 (2006).
 [3] R. Solanki, J. Huo, J. L. Freeouf, and B. Miner, *Appl. Phys. Lett.* **81**, 3864 (2002).

- [4] Y. F. Chan, X. F. Duan, S. K. Chan, I. K. Sou, X. X. Zhang, and N. Wang, *Appl. Phys. Lett.* **83**, 2665 (2003); A. Colli, S. Hofmann, A. C. Ferrari, C. Ducati, F. Martelli, S. Rubini, S. Cabrini, A. Franciosi, and J. Robertson, *Appl. Phys. Lett.* **86**, 153103 (2005).
- [5] U. Philipose, S. Yang, T. Xu, and H. E. Ruda, *Appl. Phys. Lett.* **90**, 063103 (2007).
- [6] U. Philipose, T. Xu, S. Yang, P. Sun, H. E. Ruda, Y. Q. Wang, and K. L. Kavanagh, *J. Appl. Phys.* **100**, 084316 (2006).
- [7] F. Glas, J.-Ch. Harmand, and G. Patriarche, *Phys. Rev. Lett.* **99**, 146101 (2007).
- [8] L. Malikova, W. Krystek, F. H. Pollak, N. Dai, A. Cavus, and M. C. Tamargo, *Phys. Rev. B* **54**, 1819 (1996).
- [9] B. Xiang, H. Z. Zhang, G. H. Li, F. H. Yang, F. H. Su, R. M. Wang, J. Xu, G. W. Lu, X. C. Sun, Q. Zhao, and D. P. Yu, *Appl. Phys. Lett.* **82**, 3330 (2003).
- [10] T. M. Schmidt, *Appl. Phys. Lett.* **89**, 123117 (2006).
- [11] A. Polimeni, M. Capizzi, Y. Nabetani, Y. Ito, T. Okuno, T. Kato, T. Matsumoto, and T. Hirai, *Appl. Phys. Lett.* **84**, 3304 (2004); B. A. Weinstein, T. M. Ritter, D. Strachan, M. Li, H. Luo, M. Tamargo, and R. Park, *phys. stat. sol. (b)* **198**, 167 (1996).